

Ultra-low emissions of a heavy-duty engine powered with oxymethylene ethers (OME) under stationary and transient driving conditions

Alexander D Gelner¹ , Harald A Beck², Christian Pastoetter²,
Martin Härtl¹ and Georg Wachtmeister¹

Abstract

Polyoxymethylene dimethyl ethers (OME) are promising candidates as substitutes for fossil diesel fuel. A regenerative electricity-based production, using captured airborne carbon dioxide (CO₂) and hydrogen (H₂) from water electrolysis as reactants, provides a valuable contribution to the energy transition in mobile applications. Besides the possibility of carbon-neutral production, OME offer the advantage of a sootless combustion, which resolves the trade-off between soot and nitrogen oxides (NO_x) emissions, and supports the efforts of air pollution control. While the emission behaviour of OME-powered diesel engines in raw exhaust has been studied extensively, interactions between this exhaust and components of the after-treatment system are mainly unknown. This study contains investigations conducted using a urea dosing variation (alpha titration) on a heavy-duty engine in combination with a system for selective catalytic reduction (SCR). These investigations showed a lower NO_x reduction efficiency in OME operation in partial load operation compared with the one in fossil diesel operation. This can be attributed, among other reasons, to lower exhaust temperatures in OME operation. However, the high tolerance of OME to exhaust gas recirculation (EGR) compensates for this disadvantage because of the reduction of the raw NO_x emission level. The difference in SCR efficiency disappeared at a high load operation point. Additionally, the alpha titration revealed, that urea dosing decreases formaldehyde emission in the SCR system. A pre-conditioned WHSC and WHTC cycle demonstrated the potential of an OME engine with after-treatment in the form of a twin-dosing SCR system for ultra-low emissions. For the specific evaluation of the emissions during these test cycles, this study contains the detailed calculation of the required factors – so-called ‘u-values’ – for OME exhaust according to the technical standard UN/ECE R49.

Keywords

OME, POMDME, internal combustion engine, exhaust after-treatment, SCR, alternative fuels, emissions, test cycles, WHSC, WHTC

Date received: 30 May 2021; accepted: 1 September 2021

Introduction

Climate change creates the need for reduction of anthropogenic carbon dioxide (CO₂) emissions.¹ In the transportation sector, alternative fuels based on biomass or an electricity-based synthesis (so-called e-fuels) may play an important role in the transition towards sustainable mobility solutions.² Starting with CO₂, the successive hydrogenation via hydrogen (H₂) from water electrolysis enables the formation of several hydrocarbon compounds with different oxidation stages. Among others, these include oxygenates such as aldehydes, ketones, alcohols, esters and ethers, as well as paraffinic fuels in general. These ideally carbon-neutrally

produced fuels even enable a decrease in the greenhouse gas emissions of existing internal combustion engines. In addition, it is possible to use current storage and distribution infrastructure.³ While some e-fuels show a similar combustion behaviour to their fossil counterpart, other alternatives provide advantages such as a

¹Technical University of Munich (TUM), Munich, Germany

²MAN Truck & Bus SE, Nuremberg, Germany

Corresponding author:

Alexander D Gelner, Technical University of Munich, Schragenhofstraße 31, 80992 Munich, Germany.
Email: gelner@lvk.mw.tum.de

lower emission of pollutants. For diesel engines, many studies focus on long-chain polyoxymethylene dimethyl ethers (OME) as a blend candidate or even a substitute for fossil diesel.⁴ They meet the requirements of both a carbon-neutral production,^{5,6} and of air pollution control because the combustion in a diesel engine is soot-free.^{7–12} The lack of intramolecular C–C bonds suppresses the formation of soot precursors like acetylene and polycyclic aromatic hydrocarbons¹³ and therefore resolves the trade-off between soot and nitrogen oxide (NO_x) emissions. For this reason, OME show a high tolerance against exhaust gas recirculation (EGR) for an inner-engine NO_x reduction.¹⁴ Even a stoichiometric operation without an increase of soot emission is possible.¹² While the emission behaviour of a diesel engine powered by short chain^{15–17} and long-chain^{9,11,12} OME has been studied sufficiently, interactions with after-treatment systems (ATS) are still somewhat unknown. Münz et al.¹⁸ investigated the potential of a three-way-catalyst (TWC) on a single-cylinder research engine, powered with short-chain OME₁. Pöllmann et al.¹⁹ studied the combination of a DOC and a TWC with long-chain OME in stoichiometric operation on a single-cylinder research engine. Studies on long-chain OME on complete systems, consisting of a full engine in combination with state-of-the-art ATS including a diesel oxidation catalyst (DOC), a diesel particulate filter (DPF) and a system for selective catalytic reduction (SCR) of NO_x emissions, are limited to passenger car systems.^{20,21} They focus on regulated emissions in real driving cycles, but not on different effectiveness of ATS components. Gelner et al.²² demonstrated the contrary behaviour of fuel oxidation between OME and fossil diesel on a DOC of a heavy-duty engine, but focused on fuel dosing for after-treatment system heating. An additional study will evaluate the filtration activity of a DPF on a heavy-duty engine with ATS powered by OME, as well as the volatile and non-volatile particle size distribution and the effect of urea dosing on particle emissions.²³ The NO_x reduction effectiveness of a SCR system on a lean-operated OME engine is still unknown. An incomplete combustion of OME produces formaldehyde (CH₂O),¹² which is toxic to the human body.²⁴ CH₂O also occurs in the exhaust gas composition of lean biogas engines²⁵ and several research studies provide information about the interactions of CH₂O in the ATS of these engines,^{26,27} or in general.²⁸ Besides the oxidation on a DOC,^{17,22} OME-powered diesel engines have not been studied sufficiently in this field. For this reason, this study observes the connection between urea dosing and a decrease in CH₂O in the SCR system of a heavy-duty engine, using a urea dosing variation, the so-called alpha titration. Moreover, a parallel investigation points out the NO_x reduction efficiency of the SCR system in OME and fossil diesel operation. Pre-conditioned stationary and transient test cycles demonstrate the potential of a heavy-duty OME engine with a twin-dosing SCR

Table 1. Physico-chemical properties of the tested fuels.

	Diesel	OME
Cetane number	> 51	69
Lower heating value in MJ/kg	42.6 ³⁰	19.2
Boiling range in °C	170–390 ³⁰	145–242
Flash point in °C	> 55	65
Density in kg/m ³	820–845	1,057
Oxygen content in % (w/w)	0–1 ³¹	45
	(with max. 7% (v/v) FAME)	
Volumetric diesel equivalent ratio	1	1.75
Sulphur content in ppm	< 10	< 5
Kinematic viscosity in mm ² /s	2.0–4.5	1,082
Lubricity – HFRR at 60°C in µm	≤ 460	320
Formaldehyde content in mg/kg	–	233

ASG Analytik-Service AG measured the values of OME. The values of diesel are from the standard EN 590,³² except for the LHV and boiling range, which are from Lautenschütz et al.³⁰ and the oxygen content, with the calculation using values from Hoekman et al.³¹ This calculation assumes that the FAME content consists of oleic acid.

after-treatment system with a focus also on unregulated pollutant emissions.

Methodology

Tested fuels

Polyoxymethylene dimethyl ethers (OME) are oligomers with the structure CH₃–O–(CH₂O)_{*n*}–CH₃. *n* as the amount of oxymethylene groups is often used to abbreviate the respective molecule or a mixture of different OME. For example, OME_{3–6} refers to a mixture of OME with three, four, five and six oxymethylene groups. In this study, the fuel used for the experiments contains various OME_{*n*} with major percentages of *n* = 3–6 (OME₃: 58%, OME₄: 29%, OME₅: 10%, OME₆: 2%). Additionally, the fuel contains 300 mg/kg each of butylated hydroxytoluene (BHT) as an antioxidant and a flow improver as additives. The mixture fulfils the standard M DIN TS 51699 for OME fuel²⁹ and will be simply abbreviated to OME in the following. For reference, diesel describes fossil fuel with a maximum content of 7% (v/v) fatty acid methyl esters (FAME) according to the standard EN 590³². Table 1 compares the physico-chemical properties of the fuels investigated. ASG Analytik-Service AG provided the OME fuel used and measured the values of the properties. Appendix Table A1 contains the respective standard of the measurement method used to determine each value. The values for diesel are largely from the fuel EN 590 standard. Where the standard does not provide information about a specific property, this value is taken from Lautenschütz et al.³⁰ The calculation of the oxygen content is based on the assumption that the FAME content consists of oleic acid, with the respective values from Hoekman et al.³¹

The OME mixture used contains about 45% (w/w) oxygen. This reduces the lower heating value (LHV) of

the fuel by a factor of 2.2 compared to fossil diesel. However, the higher density of OME compensates this in part, at a volumetric diesel equivalent ratio of

$$\frac{LHV_{Diesel} \cdot \rho_{Diesel}}{LHV_{OME} \cdot \rho_{OME}} \cong 1.75. \quad (1)$$

The Cetane number of OME exceeds the requirements of the EN 590 standard, which is noticeable from an excellent ignitability, proven in previous studies.^{12,33} The boiling range is similar to diesel, but with an initial boiling start and end at lower temperatures. The flash point of the OME mixture surpasses the value of EN 590. This allows the mixture to be stored and distributed in a similar way to fossil diesel. The lubricity of OME exceeds the requirement of the standard. However, the kinematic viscosity of OME is below the specification interval of the EN 590 standard. The sulphur content of OME is lower than 5 parts per million (ppm) and therefore reaches the lower limit of the determination standard for this value. Since formaldehyde is a reactant in the synthesis process of OME,⁶ the fuel tested contains an amount of 233 mg/kg. The addition with BHT prevents OME from decomposing, which results in increasing amounts of CH₂O in the fuel.

Test engine and after-treatment system

The characterisation of the behaviour of an SCR system in OME operation takes place on an MAN D2676LF51 heavy-duty six-cylinder engine. The engine has two modifications in OME operation: On the one hand, the high-pressure pump has adapted seals, in order to avoid incomparability of the sealing material in diesel operation, because both fuels differ in chemical polarity. On the other hand, the injectors in OME operation have higher nozzle flow rates in order to compensate for the reduced LHV. This is necessary to avoid longer injection durations on high-load points, which cause reduced efficiency due to an increase in the combustion duration.^{33,34} Longer injection durations may also result in interactions between the fuel jet and the lubricating film when the piston reveals the liner during downward movement. Furthermore, the higher nozzle flow rate enables rail pressure to be reduced at low- and medium-load points, which results in lower NO_x emissions.^{12,17} Table 2 shows the properties of the test engine used.

VT Vitesco Technologies Emitec GmbH provided the after-treatment system in this study. The system is modular, which allows several components to be removed or added. Table 3 contains the properties of the ATS components in downstream order of the construction. The so-called e-DOC contains a heating disc in front of the coated structure of the DOC for electrical heating. However, the experiments in this paper do not make use of this option since they focus on the behaviour of the SCR system and emissions in pre-

Table 2. Properties of the test engine MAN D2676LF51.

Number of cylinders	6 (inline)
Bore	126 mm
Stroke	166 mm
Displacement	12,419 cm ³
Compression ratio	18:1
Power	294 kW
Number of valves per cylinder	4 (2 inlet/2 exhaust)
Charge	Two-stage waste-gate turbocharger
Exhaust gas recirculation	High-pressure and cooled
Injection system	Common rail (max. 1,800 bar)
Hydraulic nozzle flow rate	Diesel: 1,300 cm ³ /30 s (at 100 bar) OME: 1,835 cm ³ /30 s (at 100 bar)

The injectors in OME operation have a higher nozzle flow rate to reduce the combustion duration at high load points.

conditioned test cycles. The system has two positions at which a doser injects the reducing agent for the SCR reaction in form of aqueous urea solution, which leads to the designation 'twin-dosing design'. This injection happens in a so-called Universal Decomposition Pipe (UDP). The conversion of urea to ammonia (NH₃) takes place in the downstream component, a titanium dioxide (TiO₂) coated hydrolysis catalyst.³⁵ Downstream, a copper-zeolite (CuZe) SCR catalyst reduces NO_x with the reducing agent NH₃.³⁶ For the demonstration using the test cycles, this SCR stage contains three discs of the catalytic monoliths, resulting in a volume of 21.5 dm³. To characterise the behaviour in diesel and OME operation, this stage contains only two monolithic discs, resulting in a volume of 14.3 dm³. The ammonia slip catalyst (ASC) oxidises excess ammonia after the SCR system selectively. This avoids the unselective oxidation to nitrous oxide (N₂O) in the DOC placed downstream.³⁷ This DOC does not contain any heating discs. The DPF is an uncoated Cordierite wall flow filter. The second UDP is followed by a mixer for the homogenisation of the ammonia in the exhaust. This supports the hydrolysis catalyst in the decomposition of the injected urea,³⁸ since the exhaust gas temperature is lower at the second stage. The second SCR stage ideally converts remaining NO_x emissions. For the demonstration using the test cycles, this SCR stage contains four discs of the catalytic monoliths, resulting in a volume of 28.8 dm³. For the characterisation of the behaviour in diesel and OME operation, this stage contains only two monolithic discs, resulting in a volume of 14.3 dm³. This stage does not have an ASC installed. The reduction of the SCR stages to two discs each allows the catalyst behaviour to be compared between the first and second stage during the characterisation.

Test bench setup

Figure 1 shows a diagram of the test bench setup. The air from the test bench air supply passes through an

Table 3. Properties of the ATS components provided by VT Vitesco Technologies Emitec GmbH in downstream order.

Component	Catalytic coating	PGM in g/ft ³	cpa	Diameter in mm	Length in mm	Volume in dm ³	Carrier material	Carrier structure	OFA* in %
e-DOC	Pt, Pd (1:1)	35	N/A	285.8	101.5	6.51	Metal	300/600 LS	82
Hyd	TiO ₂	–	N/A	174.6	60	1.43	Metal	300/600 LSPE	89
SCR	CuZe	–	N/A	300	300	3 × 101.5	Metal	600 CS	79
ASC	Pt	3	300	300	90	6.4	Metal	E300	78
DOC	Pt, Pd (1:1)	35	300	300	150	10.6	Metal	300/600 LS	82
DPF	Uncoated	None	300	305	381	27.8	Cordierite	Symmetrical	83
Hyd	TiO ₂	–	N/A	174.6	60	1.43	Metal	300 PE	89
SCR	CuZe	–	400	300	4 × 101.5	28.8	Metal	E400	77

The value of the Platinum Group Metals (PGM) density represents the total quantity of the precious metal content. Before the experiments in this study, the ATS had a mileage of about 400 km in diesel operation.*The value of the open frontal area (OFA) is based on the following assumptions: coating of the DOC is 150 g/dm³, coating of the UDP is 60 g/dm³ and coating of the SCR is 200 g/dm³, with a wash-coat density of 1.35 g/cm³.

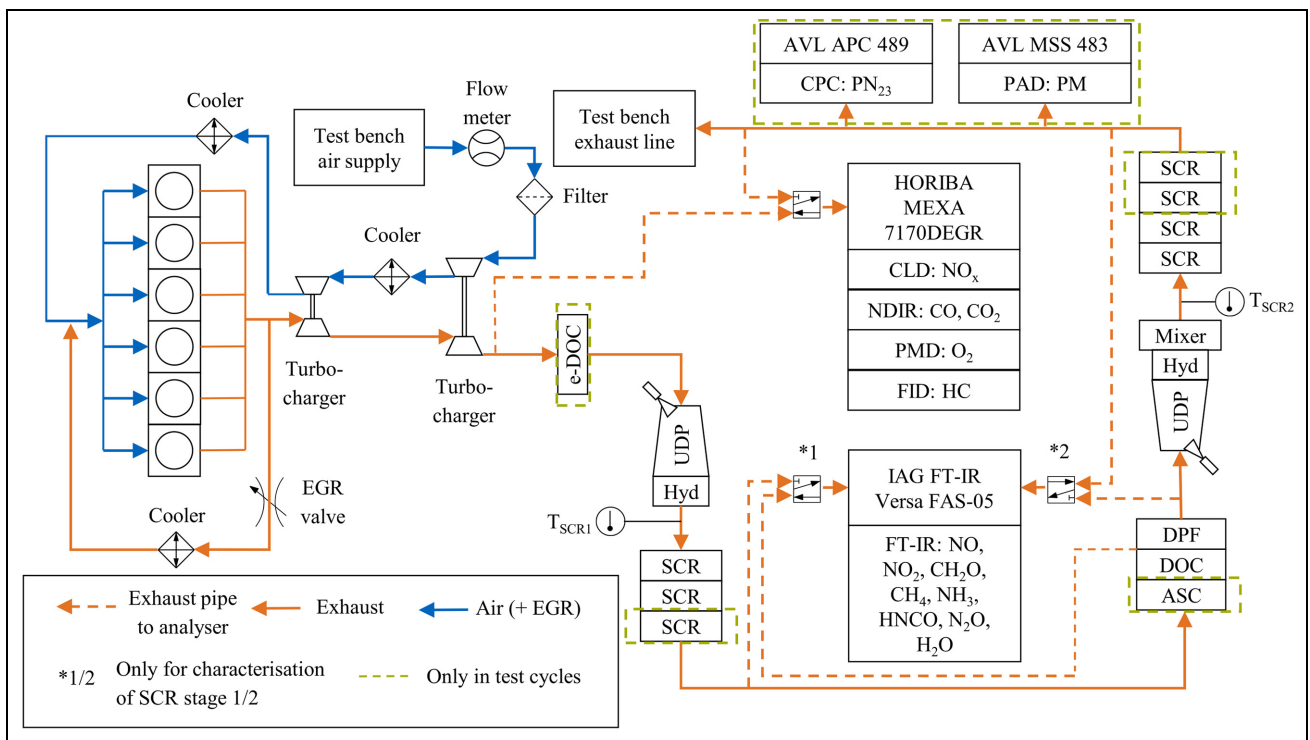


Figure 1. Test bench setup. For the characterisation of the SCR system via alpha titration, the e-DOC and ASC are removed and the SCR stages are reduced to two monolithic discs each. During the experiment with the alpha titration at the first stage, the FT-IR switches between the two sampling points marked with *1, at the second stage, it switches between the sampling points marked with *2. During the test cycles, both exhaust gas analysers extract from the tailpipe sampling position.

ABB MDM DN150 thermal dispersion mass flow meter, which determines the volumetric airflow to calculate the exhaust mass flow. Downstream, a filter avoids the contamination of the turbocharger. An intercooler reduces the temperature of the compressed air. A second turbocharger with another intercooler increases the boost pressure. The six-cylinder engine has a high-pressure EGR with intercooling, controlled by an EGR valve. Downstream of the second turbocharger, an electrically heatable DOC oxidises species in the exhaust. In this study, the heating function via

electricity remains unused. Furthermore, for the characterisation of the SCR system, this e-DOC is removed in order to generate different CH₂O emission levels in the SCR stages. The UDP contains an EMITEC ‘JC-2’ urea doser and the hydrolysis catalyst. This component provides the reducing agent NH₃ for the SCR of NO_x on the catalytic surface of the following SCR stage. During the test cycles, this stage contains three monolithic discs, while during the alpha titration, the stage is reduced to two discs. The ASC downstream of this stage also is not equipped during the alpha titration. A

second DOC also oxidises species in the exhaust, while the DPF filters particles. The second UDP is equipped with an EMITEC 'A²-8' urea doser. An EMITEC 'GEN V' urea dosing pump provides the delivery pressure for both dosers simultaneously. The second SCR stage contains four monolithic discs during the test cycles and two discs during the alpha titration. Two thermocouples of Type K, each downstream of the hydrolysis catalyst, enable the monitoring of the specific exhaust temperature upstream of the SCR catalysts. The HORIBA MEXA-7170DEGR exhaust gas analyser allows pollutants to be determined using the following components. A chemiluminescence detector (CLD) measures NO_x emissions; a nondispersive infrared sensor (NDIR) determines the concentration of carbon monoxide (CO). This analyser also measures the CO₂ concentration at the air intake of the cylinder head and downstream of the engine in order to determine the EGR rate. A paramagnetic detector (PMD) is used for the determination of the oxygen content and a flame ionisation detector (FID) displays the concentration of hydrocarbon emissions (HC) in the exhaust. The specific term of HC emissions is used for the emissions displayed by the FID in this study according to the technical standard UN/ECE Regulation No. 49.³⁹ When a comparison of this respective value takes place between diesel and OME operation, it is important to consider that the specific response factor of the partially oxidised fuel fragments in OME operation may be lower than in diesel operation because they are assumed to contain mostly oxygen.⁴⁰⁻⁴³ The measurement device has two sampling points, located downstream of the second turbocharger and tailpipe, which means downstream of the second SCR stage. A 3/2-directional control solenoid valve makes it possible to switch between these sampling points. An IAG Versa FAS-05 Fourier-transform infrared spectrometer (FT-IR) is calibrated to determine specific emissions monitored in previous studies.^{12,16} These are methane (CH₄) and formaldehyde (CH₂O). Additionally, the device measures NH₃, NO and nitrogen dioxide (NO₂), as well as isocyanic acid (HNCO) because of its health effects^{44,45} and its function as pre-cursor of deposits due to the incomplete hydrolysis of urea in the SCR system. The device also determines nitrous oxide (N₂O) because of its climate relevance.¹ Moreover, the FT-IR enables the measurement of the water (H₂O) content in the exhaust gas. The method implemented does not include the determination of the species hydrogen cyanide (HCN), which Zengel et al.²⁷ and Elsener et al.²⁸ observed during the NO_x removal via SCR with NH₃ in the presence of CH₂O. Nevertheless, during the test cycles a recording of the specific FT-IR spectra enabled a retrospective evaluation. Therefore, the test runs of the test cycles include this respective emission value and additionally values of OME_n emissions. The sampling points of the FT-IR differ between the test runs for characterisation of the first and second SCR stage. For the first stage, the points are located

downstream of the first SCR stage and downstream of the DOC, while for the second stage, they are located downstream of the DPF and tailpipe. For both setups, another 3/2-way solenoid valve enables switching during the experiment. During the test cycles, an AVL Advanced Particle Counter 489 (APC) determines the particle number (PN) emission with a condensation particle counter (CPC) and a sampling system according to the requirements of the Particle Measurement Programme.⁴⁶ An AVL Microsoot Sensor 483 (MSS) determines the soot mass, using a photoacoustic detector (PAD).⁴⁷ This value is representatively referred to as Particulate Matter (PM) in the following, since the aim is to highlight the soot reduction potential of OME. However, it is important to take into account that this value contains only black carbon in this study.

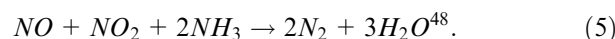
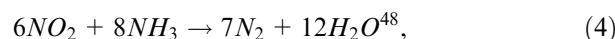
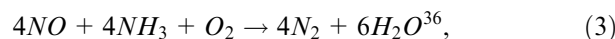
In order to determine the fuel mass flow, the fuel supply system has a DFM DR 50.02 impeller counter. The value of this device and the flow meter in the air path of the test bench add up to the value of the exhaust mass flow according to the following formula:

$$\dot{m}_{Exh} = \dot{V}_{Fuel} \cdot \rho_{Fuel} + \dot{m}_{Air}. \quad (2)$$

While the mass flow meter in the air path provides this value directly, the impeller counter provides only a volumetric flow. Therefore, this figure must be multiplied by the density of the respective fuel. In OME operation, the value from Table 1 is used. In diesel operation, the reference value of the density is 835 kg/m³.

Alpha titration and operating points

The characterisation of the SCR system in OME and diesel operation uses an alpha titration. α describes the ratio of the injected amount of urea and the required amount for the total removal of the present NO_x concentration in the exhaust. Alpha titration investigates the conversion efficiency of the system by a successive increase of α . The main reactions inside the SCR system are as follows:



Reaction (3) is designated as Standard-SCR, reaction (4) is designated as NO₂-SCR and reaction (5) is designated as Fast-SCR. However, since the NO₂/NO_x ratio rarely surpasses 50% even after the NO has been oxidised inside the DOC, Standard-SCR and Fast-SCR are assumed to account for the majority of the reactions. In that case, the stoichiometric ratio of NH₃ to NO_x is assumed to be 1 to 1 in this work. Besides these main reactions, further chemical processes happen as side reactions inside the SCR system, leading to the formation of ammonium nitrate at temperatures below 180°C⁴⁸ and N₂O.⁴⁹ These are neglected in the

Table 4. Operating points for the alpha titration.

Fuel	Diesel			OME		
	L1	L2	L3	L1	L2	L3
Engine speed in rpm	1,200	1,100	2,000	1,200	1,100	2,000
Break mean effective pressure in bar	8	18	8	8	18	8
Rail pressure in bar	1,330	1,190	1,800	1,150	990	1,640
λ	1.6	1.4	2.3	1.8	1.5	1.9
EGR rate in % (w/w)	32	20	33	32	18	43
T_{SCR1} in °C	320	400	290	280	365	260
T_{SCR2} in °C	290	370	275	260	345	250
\dot{m}_{Exh} in kg/h	465	800	1,070	525	870	1,040
sv in l/h	25,200	43,270	57,870	28,390	47,050	56,245
$NO_{x,Engine,out}$ in ppm (CLD)	380	1,075	460	240	660	235
NO_2/NO_x upstream of SCR ₂	0.51	0.42	0.30	0.30	0.35	0.24
CH ₂ O upstream of SCR ₁ in ppm	0	0	0	25	17	22
CH ₂ O upstream of SCR ₂ in ppm	0	0	0	12	1	11

The engine lambda probe determines the air-fuel ratio λ . The gravimetric EGR rate is calculated via the CO₂ concentration upstream and downstream of the engine, determined by the NDIR. The calculation of the space velocity (sv) uses the exhaust mass flow according to formula (2), the volume of the SCR catalyst with two monolithic discs according to Table 3 and the density of exhaust gas of 1.293 kg/m³ according UN/ECE R49.³⁹ The CLD determines the value of the engine-out NO_x emissions. The NO₂/NO_x ratio upstream of SCR₁ is lower than 1% at every operating point.

calculation of the amount of urea required during the alpha titration. Depending on the desired α , the urea mass flow is calculated as follows:

$$\dot{m}_{Urea} = \frac{\phi_{NO_x} \cdot \dot{m}_{Exh} \cdot M_{Urea}}{w_{Urea, AdBlue} \cdot \rho_{Exhaust} \cdot V_m \cdot r_{NH_3, Urea}} \cdot \alpha. \quad (6)$$

ϕ_{NO_x} describes the respective value of the volumetric NO_x concentration determined by the CLD in ppm. \dot{m}_{Exh} is the exhaust mass flow according to formula (2). M_{Urea} is the molar mass of urea, assumed to be 60.06 g/mol.⁵⁰ $w_{Urea, AdBlue}$ describes the mass fraction of urea within the solution used, marked as AdBlue®, which is 32.5%.⁵¹ $\rho_{Exhaust}$ is the density of the exhaust gas, estimated as 1.293 kg/m³ according to UN/ECE R49.³⁹ V_m describes the molar volume of an ideal gas with a value of 22.414 l/mol and $r_{NH_3, Urea}$ is the molar ratio of NH₃ in urea, with a value of 2.

The alpha titration starts with an α of 0.8. Before the test procedure starts, the SCR system is purged at operating point L2. The successive increase of α happens without the SCR system being cleared out. After a stationary operating status with fluctuations less than 5 ppm of NO_x emission value has been reached at both sampling points, the recording is taken three times at 1 Hz over 30 s. On the other hand, a switch to another operating point includes the cleaning process. If the value of the NH₃ concentration downstream of the SCR exceeds 10 ppm, the titration ends for this operating point. The experiments start with the characterisation of the system in diesel operation. First, the alpha titration takes place at the first SCR stage with the FT-IR sampling points switched to the specific location pointed out in Figure 1. During titration, the urea doser of the second stage is switched off. The characterisation uses three stationary operating points in the respective order of their enumeration, as Table 4 shows. The alpha

titration in diesel operation happens twice in order to evaluate on reproducibility.

The space velocity sv results from

$$sv = \frac{\dot{m}_{Exh}}{\rho_{Exh} \cdot V_{SCR}}. \quad (7)$$

After the characterisation of the first SCR stage, the experiment continues with the second stage, combined with the change of the sampling positions of the FT-IR. During these test runs, the first urea doser remains unused. For the switch from diesel to OME operation, a flush of the fuel system and several test cycles remove diesel residues. Moreover, the injector configuration changes to a setup with higher nozzle flow rates in OME operation. Additionally, the DPF is regenerated in an oven at 500°C for 6 h, as the DPF built up a soot layer in diesel operation. The SCR system is characterised in OME operation in the same chronological order as in diesel operation, starting with the first stage after a purge run. Table 4 provides the parameters of the operating points in diesel and OME operation. L1 represents an operating point with an effective power of 100 kW, L2 is a high-load point at moderate engine speed and L3 represents an operating point with a high space velocity due to high engine speed in combination with a low exhaust temperature. The exhaust temperatures upstream of the SCR stages are lower in OME operation for every operating point, while the space velocity is higher, except for L3. However, the exhaust temperatures exceed the light-off temperature of CuZe-catalysts.⁵² The higher space velocity in OME operation is due to the higher fuel mass flow, which is necessary to compensate for the lower LHV. This, in turn, ensures a higher intake air mass flow rate due to a higher enthalpy flow rate through the turbine of the turbochargers. The engine's

lambda probe determines the air-fuel-ratio λ . The adjustment of λ happens via EGR rate, which influences the intake air flow. The NO_2/NO_x ratio in the raw exhaust is $< 1\%$ for every operating point with both fuels. For this reason, the Fast-SCR reaction plays no role in the NO_x reduction at the first SCR stage.

Test cycles

The test cycles used to demonstrate the potential of the system presented for low pollutant emissions are the World Harmonized Stationary Cycle (WHSC) and the World Harmonized Transient Cycle (WHTC), in accordance with UN/ECE Regulation No. 49 (R49).³⁹ Contrary to the requirements of this regulation, the test cycles in this study start after pre-conditioning at the operating point *L2*. This measure replaces the pre-conditioning before the WHSC according to R49 and the cold run of the WHTC. Since the modular after-treatment system consists of the monolithic discs, connected via flanges and pipes, the heat losses are higher than with standard integration in a thermally insulated silencer. Therefore, an evaluation of the emission potential in this study is limited to the pre-conditioned after-treatment system. The effects of OME on the behaviour in cold-start operation will be presented in a later publication.⁵³

Contrary to the experiments of the alpha titration, the urea dosing is active at both SCR stages during the test cycles. The dosing strategy is based on an ideal distribution between the two stages, in consideration of the temperature, the ammonia storage capacity and the determined NO_x concentrations in the exhaust.

Calculation of *u*-values in OME operation

The comparison of emissions during the test cycles with the limit value stipulated by the Euro VI legislation requires the emissions to be specifically evaluated. According to UN/ECE R49, this evaluation is based on the multiplication of the integrated values over the cycle with specific factors, so-called '*u*-values', depending on the density of the exhaust. The R49 provides *u*-values for several fuels, but not for OME. Therefore, the *u*-values must be calculated in OME operation. This calculation can be used in future work for OME according to DIN SPEC 51699. The *u*-value $u_{gas,i}$ of the specific emission *i* is calculated as follows, using the density of the specific gas component $\rho_{gas,i}$ in kg/m^3 and the density of the exhaust gas ρ_e in kg/m^3 :

$$u_{gas,i} = \frac{\rho_{gas,i}}{\rho_e \cdot 1000} \quad (8)$$

While the standard R49 provides the densities of NO_x and CO, the density of HC depends on the respective fuel. It is defined as the ratio of the molar mass $M_{gas,i}$ of the component *i* in g/mol and the molar volume of an ideal gas of $22.4141/\text{mol}$ according to Avogadro's law:

$$\rho_{gas,i} = \frac{M_{gas,i}}{22.414 \frac{\text{l}}{\text{mol}}} \quad (9)$$

The values according to the fuel certificate of the OME fuel used result in a substitute molecule of $\text{C}_x\text{H}_y\text{O}_z$ with $x = 5.53$, $y = 13.45$ and $z = 4.43$. The conversion of the substitute molecule into a carbon-normalised molecule with the formula $\text{CH}_v\text{O}_\zeta$ gives rise to the molecule $\text{CH}_{2.432}\text{O}_{0.801}$. Using the atomic masses of C, H and O according to R49, the calculation of the molar mass of the normalised substitute molecule results in:

$$M_{OME} = 12.011 \frac{\text{g}}{\text{mol}} + v \cdot 1.00794 \frac{\text{g}}{\text{mol}} + \zeta \cdot 15.9994 \frac{\text{g}}{\text{mol}} = 27.2778 \frac{\text{g}}{\text{mol}} \quad (10)$$

According to formula (9), this results in a density of HC of $1.2170 \text{ kg}/\text{m}^3$ in OME operation.

The calculation of the density of the exhaust gas $\rho_{e,i}$ again requires the substitute molecule being converted into a carbon-normalised molecule with the formula $\text{CH}_{2.432}\text{O}_{0.801}$. Furthermore, the stoichiometric air to fuel ratio A/F_{st} in OME operation must also be determined. This value is calculated according from formula (11) according to R49, assuming that the fuel does not contain sulphur or nitrogen:

$$\begin{aligned} \frac{A}{F_{st}} &= \frac{138 \cdot \left(1 + \frac{v}{4} - \frac{\zeta}{2}\right)}{12.011 + 1.00794 \cdot v + 15.9994 \cdot \zeta} \\ &= 6.1088 \frac{\text{kg}}{\text{kg}} \end{aligned} \quad (11)$$

The depicted *u*-values of the emissions refer to the conditions with $\lambda = 2$ and dry air at a temperature of 273 K and a pressure of 101.3 kPa. The calculation of the exhaust gas density ρ_e for these specific conditions according to the formula

$$\rho_e = \frac{1000 + 1000 \cdot \frac{q_{mf}}{q_{mad}}}{773.4 + k_{f,w} \cdot 1000 \cdot \frac{q_{mf}}{q_{mad}}}; [\rho_e] = \frac{\text{kg}}{\text{m}^3} \quad (12)$$

requires the ratio of the fuel mass flow rate q_{mf} in kg/h to the intake air mass flow rate on a dry basis q_{mad} in kg/h . Under the condition of $\lambda = 2$, this ratio equals $\frac{1}{2 \cdot A/F_{st}}$. Furthermore, the calculation requires the fuel-specific factor of wet exhaust $k_{f,w}$, which is calculated according to the formula given:

$$k_{f,w} = 0.055594 \cdot w_v + 0.0070046 \cdot w_\zeta \quad (13)$$

w_v is the mass fraction of hydrogen in %, which is 8.99 for the OME used. w_ζ is the mass fraction of oxygen in %; for the OME used this equals 46.98 according to the atomic weights given, and the substitute molecule. Inserted in formula (13), this results in a factor of $k_{f,w} = 0.8287$.

Inserted in formula (12), the density of the exhaust in OME operation equals $1.2860 \text{ kg}/\text{m}^3$ with $\lambda = 2$, dry air at a temperature of 273 K and a pressure of 101.3 kPa.

Table 5. Calculated u -values of OME exhaust according to the formulas given in R49 and the respective u -values in diesel operation.

Fuel	ρ_e in kg/m ³	Gas		
		NO _x	CO $\rho_{\text{gas},i}$ in kg/m ³ $u_{\text{gas},i}$ ***	HC
		2.053	1.250	1.217**
Diesel (B7)*	1.2943	0.001586	0.000966	0.000482
OME	1.2860	0.001596	0.000972	0.000946

*Diesel (B7) indicates that the fuel contains up to 7% (v/v) FAME.

**For the carbon-normalised substitution molecule of OME with the molecular structure CH_{2.432}O_{0.801}.

***At $\lambda = 2$, dry air at a temperature of 273 K and a pressure of 101.3 kPa.

Table 6. Calculated u -values of OME exhaust according to the formulas given in R49.

Fuel	ρ_e in kg/m ³	Gas		
		NH ₃	N ₂ O $\rho_{\text{gas},i}$ in kg/m ³ $u_{\text{gas},i}$ **	CH ₂ O
		0.7598	1.9636	1.3396
OME	1.2860	0.000591	0.001527	0.001042

**At $\lambda = 2$, dry air at a temperature of 273 K and a pressure of 101.3 kPa.

Using formula (8), the calculated values result in the u -values for OME operation, given in Table 5.

Furthermore, this study contains a specific evaluation of the unregulated emissions NH₃, N₂O and CH₂O. Table 6 contains the u -values for these emissions in OME operation according to this calculation using formula (8) to (13).

Results and discussion

SCR efficiency

The NO_x conversion rate of an SCR system depends on several factors. A higher conversion rate is mainly caused by higher exhaust temperatures, predominant reactions according to the Fast-SCR mechanism, higher residence times on the catalytic surface and lower raw emission levels. Figure 2 contains the results of the alpha titration at both SCR stages. The procedure stops after the NH₃ slip exceeds the termination criterion of 10 ppm. The reproducibility run in diesel operation shows a maximum deviation of 5% in NO_x conversion for load point L1, 1% for L2 and 5% for L3.

At the load points L1 and L3, the SCR shows lower NO_x conversion rates in OME operation, although the engine-out NO_x level is lower. This is mainly due to lower exhaust temperatures in OME operation at both stages. The space velocity is also higher in OME operation at L1, which results in lower retention times. It is slightly lower at L3 than in diesel operation, but at the second SCR stage, the NO₂/NO_x ratio is lower, which reduces the amount of NO₂ available for the Fast-SCR reaction. Although the exhaust temperature upstream of the SCR stages is lower in OME operation, it exceeds

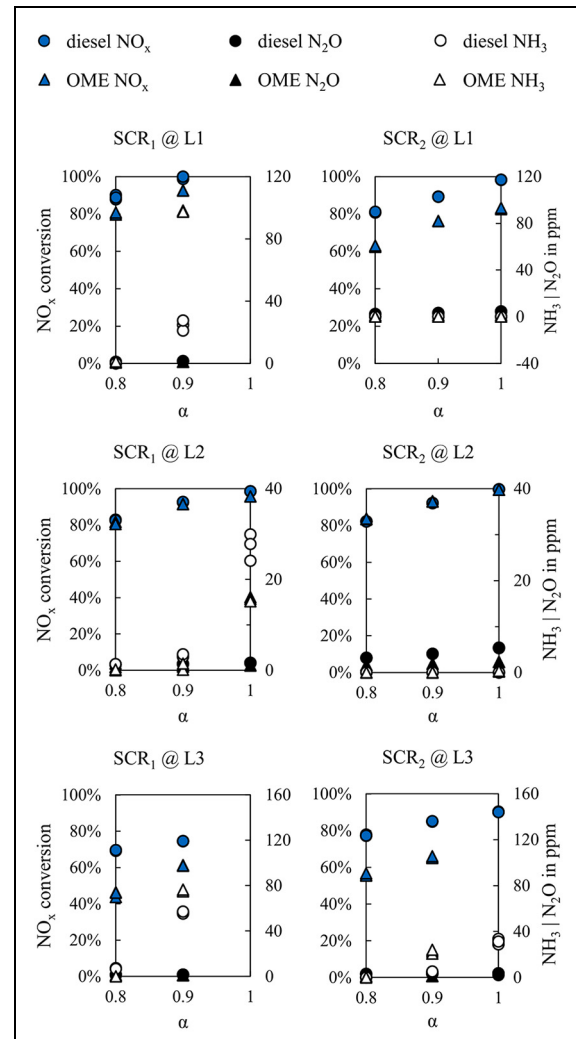


Figure 2. NO_x conversion, ammonia slip and nitrous oxide emission of the alpha titration in diesel and OME operation for both SCR stages at the operating points. The standard deviation for each point is less than 1% in NO_x conversion and 1 ppm for NH₃ and N₂O.

the light-off temperature for NO_x conversion of CuZn-catalysts.^{52,54} However, the connection between the lower exhaust temperature in OME operation and the reduced NO_x conversion is evident at both operating points. The difference is 25°C–40°C between OME and diesel operation for both SCR stages. At the high-load

point *L2*, the temperature difference does not result in a lower NO_x conversion efficiency in OME operation, nor does the higher space velocity and the lower NO_2/NO_x ratio at the second SCR stage.

Elsener et al.²⁸ revealed the reduction of NO_x conversion efficiency in the presence of 300 ppm CH_2O at a vanadium oxide SCR catalyst. Table 4 shows that the CH_2O concentration in OME operation upstream of the SCR stages is higher than 10 ppm for every operating point except *L2*, where the high exhaust temperature leads to a nearly total oxidation of CH_2O in the DOC. Therefore, the NO_x conversion rate may also be affected by the CH_2O concentration in OME operation. Because of the lower concentration levels in this work compared to in the study by Elsener et al.²⁸ this effect is assumed to be less pronounced in the presented results. Nevertheless, measures are necessary to reduce tailpipe NO_x emissions in OME operation with an SCR system according to the results presented in Figure 2. One effective method for this is a reduction of the raw NO_x emission by applying the injection^{12,34} or increasing the EGR rate.

Furthermore, Figure 2 reveals the effect of a mixer on the ammonia slip over the SCR system: While the first SCR stage without a mixer reaches the termination condition of a NH_3 slip of 10 ppm before a conversion rate of 100% at every load point, the second SCR stage does not reach this limit except for *L3*. The emission of N_2O is lower than 10 ppm at both stages with both fuels. This is due to the set α lower than 1, resulting in low ammonia storage levels. However, since it is not possible to synchronise the boundary conditions temperature, space velocity, NO_2/NO_x ratio and NO_x concentration in the raw exhaust on a heavy-duty engine, further investigations are needed to characterise the exact behaviour of the SCR system in diesel and OME operation. Nevertheless, the observed ammonia slip requires an installation of an ASC before the DOC in order to avoid the unselective oxidation of NH_3 to N_2O . Since the aim of this study is to demonstrate the emission potential of OME operation, the system for the experiments using the test cycles contains an ASC upstream of the DOC. Moreover, the soot-free combustion of OME enables a higher α at the first SCR stage, since a lower NO_2 concentration is necessary for the passive regeneration of the DPF.⁵⁵ This and an increase in the EGR rate without a subsequent soot increase compensates for the lower activity of the SCR system. However, the first stage still has to provide a NO_x slip in order to prevent the removal of stored ammonia from the second stage in dynamic operation with increasing exhaust temperature due to a NO_x conversion of 100% at the first stage.

Avoidance of hydrogen cyanide emission

Figure 3 shows the decrease of formaldehyde in the SCR system during the alpha titration. These results confirm the conclusion drawn by Bertole²⁶ and Elsener

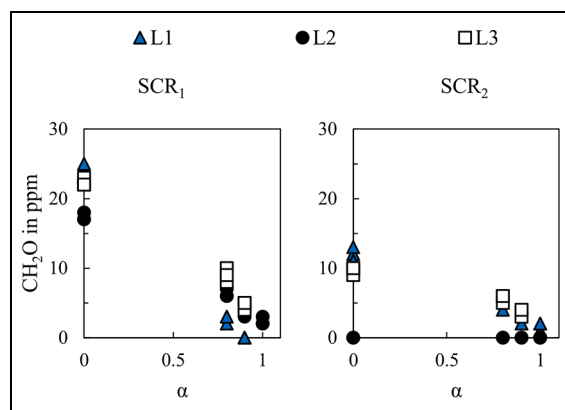


Figure 3. Reduction of formaldehyde during the alpha titration. The standard deviation for each point is less than 1 ppm.

et al.²⁸ that the injection of urea and therefore NH_3 leads to a reduction in CH_2O emission. The CH_2O concentrations upstream and downstream of the SCR systems without urea dosing differ by only 1 ppm, which means that the reduction by the catalysts without the SCR reaction is marginal. At operating point *L2*, the DOC between the two SCR stages oxidises formaldehyde completely.

Zengel et al.²⁷ and Elsener et al.²⁸ confirmed the formation of toxic⁵⁶ hydrogen cyanide in the presence of CH_2O in the SCR system. The highest yields of HCN occurred in the absence of water via formation over a formic acid pathway and at high temperatures via formation over a formaldehyde pathway at $\text{V}_2\text{O}_5/\text{WO}_3\text{-TiO}_2$ -catalysts.²⁸ As the exhaust gas of the OME engine contains water concentrations around 10% (v/v), the formation via formic acid is negligible in the present study.

In order to avoid the emission of HCN, an oxidative catalyst downstream of the SCR system is necessary to prevent HCN from entering the environment.⁵⁷ Another possibility in order to avoid HCN formation is to install an oxidative catalyst upstream of the SCR system in order to oxidise CH_2O emission. As both options require exhaust temperatures above the light-off temperature of the oxidative catalysts, the emission of HCN during cold-start operation may occur. Although the formation of ammonium nitrate prevents urea dosing during cold start operation,⁴⁹ stored ammonia⁵⁸ may play a role in the formation of HCN. An investigation into the interactions of the components of the ATS during cold-start operation is necessary and therefore forms the scope of further investigations.⁵³ For the test runs using the pre-conditioned WHSC and WHTC cycle, the additional e-DOC upstream of the first SCR stage is installed in order to oxidise CH_2O emission and prevent HCN formation.

Emissions during pre-conditioned WHSC in OME operation

Since Figure 2 reveals the lower NO_x conversion efficiency of the SCR system in OME operation, it becomes necessary to reduce the raw emission level.

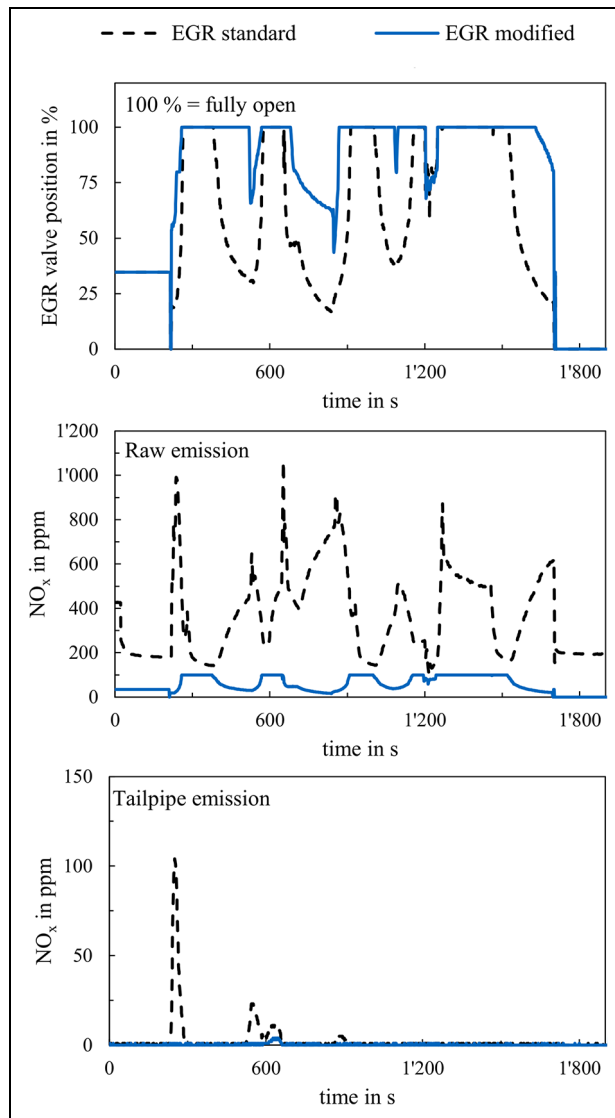


Figure 4. EGR valve position and NO_x emissions in the raw exhaust and tailpipe during the WHSC with the standard EGR application and a modified EGR application for OME operation. The engine NO_x sensor provides the raw emission values, and the CLD provides the tailpipe values.

Previous studies demonstrated the effect of high EGR rates for NO_x reduction in OME operation without an increase in soot emissions.^{11,12,14} Therefore, the following investigation is dedicated to this approach. Figure 4 compares the NO_x emissions of two EGR applications in OME operation during the WHSC. The engine NO_x sensor provides the values of raw emission levels, and the CLD provides the values of the tailpipe emission levels. Since the deviation between NO_x sensor and CLD is less than 4% in diesel operation and less than 5% in OME operation during the experiments using the alpha titration, the comparison of these two values is valid. While the EGR standard application uses the λ map of the diesel application, including the limitation of the so-called smoke limit, the EGR modified application enables the EGR valve to open faster and

Table 7. Emissions during pre-conditioned WHSC with modified EGR application.

	Result of test cycle	Euro VI limit
Emission		
CO (NDIR) in mg/kWh	0.23	4,000
NO_x (CLD) in mg/kWh	8.67	460
HC (FID) in mg/kWh	0.02	160
PM (PAD) in mg/kWh	0.027	10*
PN_{23} (CPC) in 1/kWh	9.75×10^9	8×10^{11}
NH_3 (FT-IR) in ppm	0.1	10
Unregulated emissions		
CH_4 (FT-IR) in ppm	0.0	–
CH_2O (FT-IR) in mg/kWh	0.97	–
N_2O (FT-IR) in mg/kWh	22.58	–
HNCO (FT-IR) in ppm	1.1	–
NH_3 (FT-IR) in mg/kWh	0.405	–
HCN (FT-IR) in ppm	0.1	–
$\text{OME}_{0,1,2,3,4}$ in ppm	< 1	–

*This value refers to a measurement using filter paper.

further. The modified EGR application reduces the engine's raw NO_x emissions. This reduces the level of NO_x raw emissions by approximately 46% compared to diesel operation. This leads to a nearly total conversion of NO_x in the ATS, and therefore to lower-level tailpipe emissions.

Table 7 gives the emissions of the WHSC test run using the modified EGR application. The list contains regulated emissions according to the Euro VI legislation, as well as several unregulated emissions. The Euro VI limits for heavy-duty diesel engines allow the order of magnitude of emissions in OME operation to be estimated. However, these values are not fully comparable. On the one hand, the operating point used for pre-conditioning has a higher exhaust temperature in order to compensate for the higher heat losses of the modular ATS system. On the other hand, the value of PM emission of the Euro VI legislation refers to a measurement using filter paper. In this study, a PAD determines the PM emission value, represented by the mass of soot emission.

The emission in OME operation during the WHSC is below the Euro VI limit value for every indicated species. The values are in the size range of the detection limit of the exhaust gas measurement devices used except for the PN emission. The manufacturers of the CLD, NDIR and FT-IR specify the detection limit as concentrations of around 1 ppm for every species. The unregulated emissions observed are also in this order of magnitude except for N_2O emission. Since N_2O is a greenhouse gas with massive effects on climate change,¹ further approaches to reduce this emission are necessary. Although the 100-year global warming potential of the N_2O emission during the test cycle equals less than 6 g/kWh of CO_2 equivalent with a factor of 265,¹ it is essential to avoid this emission for a climate-neutral

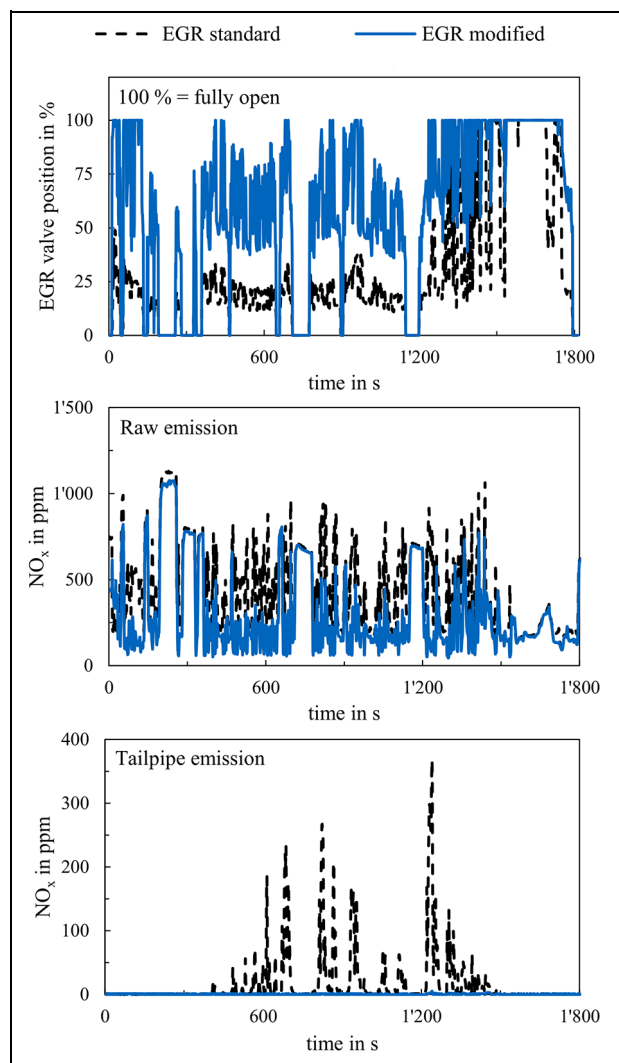


Figure 5. EGR valve position and NO_x emissions in the raw exhaust and tailpipe during the WHTC with the standard EGR application and a modified EGR application for OME operation. The engine NO_x sensor provides the raw emission values, and the CLD provides the tailpipe values.

engine operation in the case of carbon-neutrally produced OME fuel. An improvement in selectivity of the SCR catalyst is one effective means of reducing N_2O emission. The retrospective evaluation of the FT-IR spectra reveals that the emission of the test run for each OME_{0-4} is less than 1 ppm. With the ATS configuration used in this study, the emission of HCN during the test run was 0.1 ppm. The value of the HNCO emission is 1.1 ppm.

Emissions during pre-conditioned WHTC in OME operation

Figure 5 shows the NO_x emissions in raw and tailpipe exhaust using the same EGR applications as in the WHSC cycle. Similar to the results presented in Figure 4, modified EGR application for OME operation reduces the NO_x raw emissions level by

Table 8. Emissions during pre-conditioned WHTC with modified EGR application.

Emission	Result of test cycle	Euro VI limit
CO (NDIR) in mg/kWh	14.5	4,000
NO_x (CLD) in mg/kWh	4.31	460
HC (FID) in mg/kWh	18.72	160
PM (MSS) in mg/kWh	0.068	10*
PN_{23} (CPC) in 1/kWh	1.56×10^{10}	6×10^{11}
NH_3 (FT-IR) in ppm	0.1	10
Unregulated emissions		
CH_4 (FT-IR) in ppm	2.3	–
CH_2O (FT-IR) in mg/kWh	1.56	–
N_2O (FT-IR) in mg/kWh	23.64	–
HNCO (FT-IR) in ppm	1.3	–
NH_3 (FT-IR) in mg/kWh	0.277	–
HCN (FT-IR) in ppm	0.0	–
$\text{OME}_{0,1,2,3,4}$ in ppm	< 1	–

*This value refers to a measurement using filter paper.

approximately 62% compared to diesel operation. While there are several points with NO_x slip using the standard EGR application, the modified strategy enables nearly total conversion in the ATS.

Table 8 shows the results of the WHTC test run with modified EGR application in OME operation. As in the WHSC evaluation, the table also gives the limits according to the Euro VI legislation. Just like in the WHSC, a direct comparison of the results and the limit values is limited, as the pre-conditioning differs from the mandatory test procedure in the technical standard R49. Moreover, the Euro VI limit refers to a test run including a cold-start cycle and a subsequent run of the WHTC. Nevertheless, a classification of the order of magnitude is possible.

The emission in OME operation during the pre-conditioned WHTC is below the Euro VI limit value for every species indicated. Again, the values are in the size range of the detection limit of the exhaust gas measurement devices used except for the PN emission, as with the WHSC results. The unregulated emissions observed are also in this magnitude of order except for N_2O emission. Moreover, the CH_4 emission is higher in dynamic operation. In a test run with the standard EGR application, the CH_4 emission is 0 ppm. As Barro et al.⁹ and Pélerin et al.¹² previously revealed, high EGR rates, leading to a λ of lower than 1.1, result in the formation of CH_4 . Therefore, a NO_x - CH_4 trade-off replaces the resolved NO_x -soot trade-off in OME operation, especially in transient operation. Since CH_4 is another greenhouse gas,^{1,59} this has to be considered in the application of OME engines. The remaining emissions considered are in the range of the WHSC results. This demonstrates, that an OME engine with a twin-dosing ATS offers the potential of a stationary and transient operation with the lowest pollutant emissions. Due to the reduction in the level of NO_x emissions in

the raw exhaust presented, simplifications of the ATS are also considerable in order to improve the economic efficiency in the cost of tailpipe emissions. A one-stage SCR system may also be able to meet upcoming legislation standards. Furthermore, the sootless combustion enables the removal of the DPF. The effects of an OME-operated engine on the PN emission of the regulated nanoparticles with a minimum diameter of 23 nm and unregulated particle sizes form the scope of another study, in addition to the effect of the DPF and urea dosing on the tailpipe emission level of nanoparticles.²³

Conclusions and outlook

The present work contains a comparison of the efficiency of a CuZe-SCR system in operation with fossil diesel and OME. Furthermore, the investigation reveals the diminishing effect of urea dosing on formaldehyde emission in OME operation. The demonstration of a pre-conditioned WHSC and WHTC run confirm the potential for lowest pollutant emissions of an OME engine in combination with a twin-dosing after-treatment system. Furthermore, this study contains the calculation of the specific u -values for OME operation according to UN/ECE R49 for the specific emission evaluation of the test cycles. The results are summarised in the following conclusions:

- In OME operation, the exhaust gas temperatures are lower than in diesel operation. This results in a lower relative NO_x conversion efficiency in the SCR system. This does not apply for the investigated high-load point, where the efficiency is approximately equal.
- The sootless combustion of OME enables a high-EGR strategy, leading to lower NO_x emissions in the raw exhaust. This compensates for the reduced conversion efficiency. Moreover, the sootless combustion reduces the required amount of NO_2 for the continuous regeneration of the DPF, enabling a higher α at the first SCR stage in twin-dosing operation. Nevertheless, removal of stored ammonia in the second SCR stage at increasing exhaust temperatures restricts the urea dosing at the first stage.
- Urea dosing in the SCR system reduces the level of formaldehyde emission in the exhaust of OME engines. Since the literature provides information about the formation of HCN in the presence of formaldehyde and ammonia, either the removal of formed HCN by oxidative catalysts downstream of the SCR system or the previous total oxidation of CH_2O upstream of the SCR system are necessary to avoid the emission of this toxic species into the environment. During the pre-conditioned runs of the test cycles WHSC and WHTC, no emission of HCN occurred.
- With the twin-dosing after-treatment system used, regulated pollutant emissions fall within the range

of the detection limits of the exhaust gas measurement devices used during the pre-conditioned runs of the test cycles WHSC and WHTC, except for particle number emission. Nevertheless, the emission of PN with particles with a minimum diameter of 23 nm are each lower than the Euro VI limit by a double-digit factor. The ultra-low level of NO_x emission is due to the modified EGR application in OME operation, which features faster and further opening of the EGR valve. The unregulated pollutant emissions CH_2O , H₂CO, HCN and OME_n are also in the range of the detection limit.

- The emission value of the greenhouse gas N_2O requires further reduction efforts, because of its massive impact on the climate change.
- While no CH_4 emission was detected in stationary operation, several emission peaks in dynamic operation result in a minimally increased cycle result of the WHTC compared to the WHSC. A test run with the standard EGR application reveals that this is due to a brief undershoot of the λ limit of CH_4 formation. For ultra-low emissions applications, an increase in SCR performance enables higher NO_x conversion efficiencies, so the EGR application may consider the NO_x - CH_4 trade-off in dynamic operation without the disadvantage of higher NO_x tailpipe emissions. However, the lower-level NO_x emission in the raw exhaust due to the modified EGR strategy also enables the after-treatment system to be simplified, leading to lower costs, while upcoming exhaust gas legislation still may be fulfilled.

Although this study demonstrates the potential of an OME engine in combination with after-treatment for ultra-low emissions, these observations refer to an operationally warm system. Therefore, an investigation into the emission behaviour of the system used in cold-start operation is necessary in order to evaluate the system holistically. In particular, emission of HCN in cold-start operation with a temperature level of the oxidative catalysts below their respective light-off temperature requires further observation. Another study is planned with a focus on this subject.⁵³ Furthermore, the emission of nanoparticles below the regulated particle size of minimum 23 nm in the system presented, as well as the effect of the DPF and urea dosing on PN emission will be discussed in another publication.²³

Acknowledgements

The project 'Sub-Zero-Emissions Dieselmotor' was funded by the Bavarian Research Foundation (BFS) and was carried out in collaboration with MAN Truck & Bus SE, VT Vitesco Technologies Emitec GmbH, Chair of Analytical Chemistry of TUM and ASG Analytik-Service AG. Their support is gratefully acknowledged. The authors also want to thank Dr. Dieter Rothe and Dipl.-Ing. Florian Lindner (both MAN Truck & Bus SE) for their support and consultation in this study.

Author contributions

Alexander D Gelner: conceptualisation, data curation, formal analysis, investigation, methodology, project administration, validation, visualisation, writing – original draft and writing – review and editing. Harald A Beck: validation, formal analysis, data curation and writing – review and editing. Christian Pastoetter: funding acquisition, project administration and writing – review and editing. Martin Härtl: funding acquisition, project administration, supervision and writing – review and editing. Georg Wachtmeister: funding acquisition, project administration, supervision and writing – review and editing.


Declaration of conflicting interests

The authors declared no potential conflicts of interest with respect to the research, authorship, and/or publication of this article.

Funding

The authors disclosed receipt of the following financial support for the research, authorship, and/or publication of this article: The research was part of the project ‘Sub-Zero-Emissions Dieselmotor’, funded by the Bavarian Research Foundation (grant number AZ-1266-17).

ORCID iD

Alexander D Gelner  <https://orcid.org/0000-0001-9628-798X>

References

- Pachauri RK and Meyer L (eds.). *Climate change 2014: synthesis report [longer report]*. Geneva, Switzerland: Intergovernmental Panel on Climate Change, 2015.
- Schemme S, Breuer JL, Köller M, et al. H₂-based synthetic fuels: a techno-economic comparison of alcohol, ether and hydrocarbon production. *Int J Hydrogen Energy* 2020; 45: 5395–5414.
- Gray N, McDonagh S, O’Shea R, Smyth B and Murphy JD. Decarbonising ships, planes and trucks: an analysis of suitable low-carbon fuels for the maritime, aviation and haulage sectors. *Adv Appl Energy* 2021; 1: 100008.
- Schemme S, Samsun RC, Peters R and Stolten D. Power-to-fuel as a key to sustainable transport systems – an analysis of diesel fuels produced from CO₂ and renewable electricity. *Fuel* 2017; 205: 198–221.
- Centi G and Perathoner S. Opportunities and prospects in the chemical recycling of carbon dioxide to fuels. *Catal Today* 2009; 148: 191–205.
- Held M, Tönges Y, Pélerin D, Härtl M, Wachtmeister G and Burger J. On the energetic efficiency of producing polyoxymethylene dimethyl ethers from CO₂ using electrical energy. *Energy Environ Sci* 2019; 12: 1019–1034.
- Pellegrini L, Marchionna M, Patrini R, et al. Emission performance of neat and blended polyoxymethylene dimethyl ethers in an old light-duty diesel car. SAE technical paper 2013-01-1035, 2013.
- Iannuzzi SE, Barro C, Boulouchos K and Burger J. Combustion behavior and soot formation/oxidation of oxygenated fuels in a cylindrical constant volume chamber. *Fuel* 2016; 167: 49–59.
- Barro C, Parravicini M, Boulouchos K and Liati A. Neat polyoxymethylene dimethyl ether in a diesel engine; part 2: exhaust emission analysis. *Fuel* 2018; 234: 1414–1421.
- Damyantov A, Hofmann P, Geringer B, Schwaiger N, Pichler T and Siebenhofer M. Biogenous ethers: production and operation in a diesel engine. *Automot Engine Technol* 2018; 3: 69–82.
- Omari A, Heuser B, Pischinger S and Rüdinger C. Potential of long-chain oxymethylene ether and oxymethylene ether-diesel blends for ultra-low emission engines. *Appl Energy* 2019; 239: 1242–1249.
- Pélerin D, Gaukel K, Härtl M, Jacob E and Wachtmeister G. Potentials to simplify the engine system using the alternative diesel fuels oxymethylene ether OME₁ and OME_{3–6} on a heavy-duty engine. *Fuel* 2020; 259: 116231.
- Ogawa H, Miyamoto N and Yagi M. Chemical-kinetic analysis on PAH formation mechanisms of oxygenated fuels. SAE technical paper 2003-01-3190, 2003.
- Pellegrini L, Marchionna M, Patrini R, et al. Combustion behaviour and emission performance of neat and blended polyoxymethylene dimethyl ethers in a light-duty diesel engine. SAE technical paper 2012-01-1053, 2012.
- Ogawa H, Nabi N, Minami M, et al. Ultra low emissions and high performance diesel combustion with a combination of high EGR, three-way catalyst, and a highly oxygenated fuel, dimethoxy methane (DMM). SAE technical paper 2000-01-1819, 2000.
- Härtl M, Seidenspinner P, Jacob E and Wachtmeister G. Oxygenate screening on a heavy-duty diesel engine and emission characteristics of highly oxygenated oxymethylene ether fuel OME₁. *Fuel* 2015; 153: 328–335.
- Pélerin D, Gaukel K, Härtl M, et al. Nitrogen oxide reduction potentials using dimethyl ether and oxymethylene ether in a heavy-duty diesel engine. SAE technical paper series 2020-01-5084, 2020.
- Münz M, Töpfer D, Mokros A, et al. Oxygenate fuel in a diesel engine – is a CI engine capable of lambda 1? In: Liebl J and Beidl C (eds) *Internationaler Motorenkongress 2017*. Wiesbaden, Germany: Springer Fachmedien Wiesbaden, 2017, pp.457–472.
- Pöllmann S, Härtl M and Wachtmeister G. Potentials of the synthetic diesel fuel oxymethylene ether under stoichiometric conditions with aftertreatment. Manuscript in preparation.
- Münz M, Mokros A, Töpfer D and Beidl C. OME – assessment of particle emissions in real driving conditions. *MTZ Worldw* 2018; 79: 16–21.
- Münz M, Mokros A and Beidl C. Analysis of two engine configurations using OME as a potential CO₂-neutral and low emission diesel substitute. In: Liebl J, Beidl C and Maus W (eds) *Internationaler Motorenkongress 2019*. Wiesbaden, Germany: Springer Fachmedien Wiesbaden, 2019, pp.369–384.
- Gelner AD, Pastoetter C, Beck HA, et al. Fuel dosing on a diesel oxidation catalyst for after-treatment system heating on a heavy-duty engine powered by polyoxymethylene dimethyl ethers. SAE technical paper 2020-01-2157, 2020.
- Gelner AD, Rothe D, Irwin M, et al. Particle emissions of a heavy-duty engine powered by polyoxymethylene dimethyl ethers (OME): volatile and nonvolatile particle size distributions and PN-emissions in test cycles. 2021. Manuscript in preparation.
- Fischer MH. The toxic effects of formaldehyde and formalin. *J Exp Med* 1905; 6: 487–518.

25. Bauer M and Wachtmeister G. Formation of formaldehyde in lean-burn gas engines. *MTZ Worldw* 2009; 70: 50–57.
26. Bertole C. Formaldehyde oxidation over emission control catalysts. SAE technical paper 2018-01-1274, 2018.
27. Zengel D, Koch P, Torkashvand B, Grunwaldt JD, Casapu M and Deutschmann O. Emission of toxic HCN during NO_x removal by ammonia SCR in the exhaust of lean-burn natural gas engines. *Angew Chem Int Ed Engl* 2020; 59: 14423–14428.
28. Elsener M, Nuguid RJG, Kröcher O and Ferri D. HCN production from formaldehyde during the selective catalytic reduction of NO_x with NH₃ over V₂O₅/WO₃-TiO₂. *Appl Catal B* 2021; 281: 119462.
29. DIN/TS 51699 – Fuels – Polyoxymethylene dimethyl ether (OME).
30. Lautenschütz L, Oestreich D, Seidenspinner P, Arnold U, Dinjus E and Sauer J. Physico-chemical properties and fuel characteristics of oxymethylene dialkyl ethers. *Fuel* 2016; 173: 129–137.
31. Hoekman SK, Broch A, Robbins C, Cenicerros E and Natarajan M. Review of biodiesel composition, properties, and specifications. *Renew Sustain Energ Rev* 2012; 16: 143–169.
32. DIN EN 590:2017-10 – Automotive fuels – diesel. CEN/TC 19 WG 24, 2017. <https://www.din.de/en/getting-involved/standards-committees/nmp/publications/wdc-beuth:din21:278413784>
33. Barro C, Parravicini M and Boulouchos K. Neat polyoxymethylene dimethyl ether in a diesel engine; part 1: detailed combustion analysis. *Fuel* 2019; 256: 115892.
34. Gelner AD, Höß R, Zepf A, et al. Engine operation strategies with the alternative diesel fuel oxymethylene ether (OME): evaluation based on injection rate analyzer and 0D-/1D-simulation. *SAE technical paper 2021-01-1190*, 2021. Manuscript submitted for publication.
35. Yim SD, Kim SJ, Baik JH, et al. Decomposition of urea into NH₃ for the SCR process. *Ind Eng Chem Res* 2004; 43: 4856–4863.
36. Koebel M, Elsener M and Marti T. NO_x-reduction in diesel exhaust gas with urea and selective catalytic reduction. *Combust Sci Technol* 1996; 121: 85–102.
37. Kamasamudram K, Henry C, Currier N and Yezerets A. N₂O formation and mitigation in diesel aftertreatment systems. *SAE Int J Engines* 2012; 5: 688–698.
38. Birkhold F, Meingast U, Wassermann P and Deutschmann O. Modeling and simulation of the injection of urea-water-solution for automotive SCR DeNO_x-systems. *Appl Catal B* 2007; 70: 119–127.
39. Regulation No. 49 of the Economic Commission for Europe of the United Nations (UN/ECE)—uniform provisions concerning the measures to be taken against the emission of gaseous and particulate pollutants from compression-ignition engines and positive ignition engines for use in vehicles, 2013. Official Journal of the European Union; [https://eur-lex.europa.eu/legal-content/EN/TXT/PDF/?uri=CELEX:42013X0624\(01\)&from=DE](https://eur-lex.europa.eu/legal-content/EN/TXT/PDF/?uri=CELEX:42013X0624(01)&from=DE).
40. Scanlon JT and Willis DE. Calculation of flame ionization detector relative response factors using the effective carbon number concept. *J Chromatogr Sci* 1985; 23: 333–340.
41. Jorgensen AD, Picel KC and Stamoudis VC. Prediction of gas chromatography flame ionization detector response factors from molecular structures. *Anal Chem* 1990; 62: 683–689.
42. Huang Y, Ou Q and Yu W. Characteristics of flame ionization detection for the quantitative analysis of complex organic mixtures. *Anal Chem* 1990; 62: 2063–2064.
43. Wallner T. Correlation between speciated hydrocarbon emissions and flame ionization detector response for gasoline/alcohol blends. In: *ASME 2010 Internal Combustion Engine Division Fall Technical Conference*, San Antonio, TX, USA, 12–15 September 2010, pp. 119–128. ASMEDC.
44. Roberts JM, Veres PR, Cochran AK, et al. Isocyanic acid in the atmosphere and its possible link to smoke-related health effects. *Proc Natl Acad Sci U S A* 2011; 108: 8966–8971.
45. Leslie MD, Ridoli M, Murphy JG and Borduas-Dedekind N. Isocyanic acid (HNCO) and its fate in the atmosphere: a review. *Environ Sci Process Impacts* 2019; 21: 793–808.
46. Andersson J, Mamakos A and Giechaskiel B. *Particle measurement programme (PMP) heavy-duty inter-laboratory correlation exercise (ILCE_HD)*. Luxembourg: Publications Office of the European Union, 2010.
47. Beck HA, Niessner R and Haisch C. Development and characterization of a mobile photoacoustic sensor for on-line soot emission monitoring in diesel exhaust gas. *Anal Bioanal Chem* 2003; 375: 1136–1143.
48. Koebel M, Madia G and Elsener M. Selective catalytic reduction of NO and NO₂ at low temperatures. *Catal Today* 2002; 73: 239–247.
49. Forzatti P, Lietti L and Tronconi E. Nitrogen oxides removal-industrial. In: I Horváth (ed.) *Encyclopedia of Catalysis*. Hoboken, NJ: John Wiley & Sons, Inc, 2002, p.6.
50. National Center for Biotechnology Information. PubChem compound summary for CID 1176, Urea, <https://pubchem.ncbi.nlm.nih.gov/compound/Urea>. (2020 accessed 9 May 2021).
51. ISO 22241-1:2019. Diesel engines – NO_x reduction agent AUS 32.
52. Kamasamudram K, Currier N, Szailler T and Yezerets A. Why Cu- and Fe-zeolite SCR catalysts behave differently at low temperatures. *SAE Int J Fuel Lubricants* 2010; 3: 664–672.
53. Gelner AD, Pang G, Haisch C, et al. Emissions of a heavy-duty diesel engine powered with polyoxymethylene dimethyl ethers during cold start operation. Manuscript in preparation.
54. Kröcher O. Chapter 9. Aspects of catalyst development for mobile urea-SCR systems — from Vanadia-Titania catalysts to metal-exchanged zeolites. In: Granger P and Pârvulescu VI (eds) *Past and present in DeNO_x catalysis – from molecular modelling to chemical engineering*. Studies in Surface Science and Catalysis. Elsevier, 2007, pp.261–289.
55. Kandylas IP and Koltsakis GC. NO₂-assisted regeneration of diesel particulate filters: a modeling study. *Ind Eng Chem Res* 2002; 41: 2115–2123.
56. Higgins EA, Fiorca V, Thomas AA and Davis HV. Acute toxicity of brief exposures to HF, HCl, NO₂ and HCN with and without CO. *Fire Technol* 1972; 8: 120–130.
57. Kröcher O and Elsener M. Hydrolysis and oxidation of gaseous HCN over heterogeneous catalysts. *Appl Catal B* 2009; 92: 75–89.

58. Johnson TV. Review of selective catalytic reduction (SCR) and related technologies for mobile applications. In: Nova I and Tronconi E (eds) *Urea-SCR technology for deNO_x after treatment of diesel exhausts*. New York, NY: Springer, 2014, pp.3–31.
59. Etminan M, Myhre G, Highwood EJ and Shine KP. Radiative forcing of carbon dioxide, methane, and nitrous oxide: a significant revision of the methane radiative forcing. *Geophys Res Lett* 2016; 43: 12,614–12,623.

Appendix

Definitions/Abbreviations

A/F _{st}	stoichiometric air to fuel ratio	PGM	platinum group metals
ASC	ammonia slip catalyst	PM	particulate matter
ATS	after-treatment system	PN ₍₂₃₎	particle number (with a 50%-cut-off at 23 nm)
BHT	butylated hydroxytoluene	ppm	parts per million
CLD	chemiluminescence detector	q_{mad}	intake air mass flow rate on a dry basis
cp _{si}	cells per square inch	q_{mf}	fuel mass flow rate
CuZe	copper zeolite	$r_{\text{NH}_3, \text{Urea}}$	molar fraction of NH ₃ in urea
DOC	diesel oxidation catalyst	SCR	selective catalytic reduction
DPF	diesel particulate filter	sv	space velocity
EGR	exhaust gas recirculation	TiO ₂	titanium dioxide
FAME	fatty acid methyl esters	TWC	three-way catalyst
FID	flame ionisation detector	$u_{\text{gas}, i}$	u -value of the specific component i
FT-IR	Fourier-transform infrared spectrometer	UDP	Universal Decomposition Pipe
HC	hydrocarbon (determined by the flame ionisation detector)	\dot{V}_{Fuel}	fuel volume flow
HFRR	high-frequency reciprocating rig	V_{m}	molar volume of an ideal gas
LHV _(n)	lower heating value (of the component n)	V_{SCR}	volume of the SCR catalysts
$k_{f, w}$	fuel-specific factor of wet exhaust	$w_{\text{Urea, AdBlue}}$	mass fraction of urea in AdBlue [®]
\dot{m}_{Air}	air mass flow	w_{v}	mass fraction of hydrogen in %
\dot{m}_{Exh}	exhaust gas mass flow	w_{ζ}	mass fraction of oxygen in %
$M_{\text{gas}, i}$	molar mass of the component i	WHSC	World Harmonized Stationary Cycle
M_{OME}	molar mass of OME	WHTC	World Harmonized Transient Cycle
M_{Urea}	molar mass of urea	x	index of carbon atoms in the substitution molecule
\dot{m}_{Urea}	urea mass flow	y	index of hydrogen atoms in the substitution molecule
NDIR	nondispersive infrared sensor	z	index of oxygen atoms in the substitution molecule
OFA	open frontal area	α	ratio of dosed amount of urea to the required amount of urea for total conversion of the NO _x emissions
OME _(n)	polyoxymethylene dimethyl ethers (of the chain-length n)	λ	air-fuel ratio
PAD	photoacoustic detector	φ_{NO_x}	volume fraction of NO _x in the exhaust
		$\rho_{(n)}$	density (of the component n)
		ρ_{e}	exhaust gas density
		$\rho_{\text{gas}, i}$	density of the specific gas component i
		v	index of hydrogen atoms in the substitution molecule, normalised to $x = 1$

Table A1 Determined values of OME and the respective measurement method.

	Value	Method
Cetane number	68.8	DIN EN 17155: 2018
Oxygen content in % (w/w)	45.0	DIN 51732: 2014 mod.
Sulphur content in mg/kg	< 5	DIN EN ISO 20884: 2011
Lower heating value in MJ/kg	19.21	DIN 51900-2: 2003 mod.
Density (15°C at 1 bar) in kg/dm ³	1,057.1	DIN EN ISO 12185: 1997
Boiling range at 1 bar in °C	144.9–242.4	DIN EN ISO 3405: 2011
Flash point at 1 bar in °C	65.0	DIN EN ISO 2719: 2016
Cold filter plugging point in °C	–40	DIN EN 116: 2018
Cloud point in °C	–38	DIN EN 23015: 1994
Kinematic viscosity at 40°C in mm ² /s	1.082	DIN EN ISO 3104: 1999
Lubricity – HFRR at 60°C in μm	320	DIN EN ISO 12156-1: 2016
Formaldehyde content in mg/kg	233	ASG 1855 Voltammetry

ζ	index of hydrogen atoms in the substitution molecule, normalised to $x = 1$	H ₂ H ₂ O HCN	hydrogen water hydrogen cyanide (IUPAC: formonitrile)
Chemical formula		HNCO	isocyanic acid
CH ₄	methane	N ₂	nitrogen
CH ₂ O	formaldehyde (IUPAC: methanal)	N ₂ O NH ₃	nitrous oxide ammonia
CO	carbon monoxide	NO	nitric oxide
CO ₂	carbon dioxide	NO ₂	nitrogen dioxide
CO ₂	carbon dioxide	NO _x TiO ₂	nitrogen oxides titanium dioxide